

A novel miniaturized polarization-independent fiber-optic interferometer

YOU-XIANG YE^{a,b}, HAI-PING MEI^{d,*}, SHENG-HUA ZHOU^c, DA-WEI ZHANG^b, RUI-JIN HONG^b

^aCollege of Modern Science and Technology, China JiLiang University, Hangzhou 310018, China

^bSchool of Optical-electrical and Computer Engineering, University of Shanghai for Science and Technology, Shanghai, 200093, China

^cCollege of Optical and Electronic Technology, China JiLiang University, Hangzhou, 310018, China

^dKey Laboratory of Atmospheric Composition and Optical Radiation, Anhui Institute of Optics and Fine Mechanics, Chinese Academy of Sciences, Hefei, 230031, China

This paper described a novel miniaturized polarization-independent fiber-optic interferometer based on a SFOP and its application in micro-vibration measurement. Firstly, we presented a SFOP which can eliminate the polarization fading effect. Secondly, we established the hardware system of a novel miniaturized polarization-independent fiber-optic interferometer. Finally, we analyzed the fitting results of experiment data of micro-vibration measurement. The phase-shift coefficient $\Delta\phi/\Delta V$ of PZT is 9.924 rad/V and 10.286 rad/V when the voltage changes from 3.0V to 4.8V and from 0.5V to 4.0V, respectively. The error is mainly due to the hysteresis of PZT. The experimental results showed that the interferometer can be perfectly used to measure the micro-vibration.

(Received September 5, 2017; accepted February 12, 2018)

Keywords: Fiber-optic interferometer, Common-path interference, Micro-vibration measurement

1. Introduction

In traditional vibration monitoring, the acceleration sensor is widely used. However it is a contact type sensor and it must be attached to the surface of the object to be measured, which restricts its applications in many occasions such as micro-vibration measurement. The laser interferometry for vibration measurement uses a small and low energy laser beam to carry out the nondestructive non-contact measurement of the vibrating object, which solves the above problems and obtains accurate measurement results [1]. Generally, the optical vibrometer system in the form of Michelson interferometer's orthogonal space uses excessively of optical elements [2], which causes some new problems of complex structure, installation difficulties, sensitivity of environments, and so on.

Fiber-optic interferometer has great potential for application owing to its advantages, such as small size, light weight, low cost, high sensitivity, compact structure, anti electromagnetic interference and non-contact measurement [3]. In fact, the lights participating in the interference have the same polarization state for interferometric fiber-optic sensors. The visibility of interference signals output will change along with the light polarization state's change during transmission, when the interferometer is composed of ordinary low cost single-mode fiber. Especially the interference signal is zero when the polarization of the two beams is

orthogonal. The signal fading, which caused by the change of polarization state, is one of the key problems that needs to be solved in the practical application of the interferometric fiber-optic sensor [4]. There are two main methods to solve the signal fading problem as a result of polarization at present. One method is adding up to the two arms of Michelson interferometer with a Faraday rotator mirror [5], which effectively solves the fading phenomenon. However at the same time it increases the complexity of the device and reduces the stability. It is not conducive to the sensor's miniaturization and integration. The other is the use of the all-polarization-maintaining fiber, but it is expensive for developing the corresponding experimental system [6].

To solve these problems mentioned above, we presented a special polarization-independent fiber-optic interferometer based on a SFOP (special fiber-optic probe). It can almost eliminate the signal fading phenomenon for the special design of common-path interference structure [7,8], and has the advantages of miniaturization, simple and compact structure, high integration, good stability and high sensitivity characteristics.

2. Principles and structures

Taking the typical light field of amplitude division double-beam interference as an example, the intensity of the signal beam and the reference beam as follows:

$$E_1 = E_{10} \exp\{i[\omega t + \phi_s(t) + \phi_0]\} \quad (1)$$

$$E_2 = E_{20} \exp\{i[\omega t + \phi_r]\} \quad (2)$$

Where E_{10} is the amplitude of signal light, $\phi_s(t)$ is the phase modulation, ϕ_0 is the initial phase of signal light, E_{20} is the reference light field amplitude, ϕ_r is the reference phase, ω is the circular frequency of the light source.

The field distribution of interference fringes produced by two beams is

$$E(t) = \{E_{10} \exp[i(\phi_s(t) + \phi_0)] + E_{20} \exp[i\phi_r]\} \exp(i\omega t) \quad (3)$$

The corresponding intensity distribution is

$$I = I_0 \{1 + k \cos[\phi_s(t) + \phi_s - \phi_r]\} \quad (4)$$

Where I_0 is the peak intensity, the interference fringe's visibility k ($k \leq 1$) is the proportional coefficient which related with E_{10} , E_{20} and the polarization [9]. If $E_{10} = E_{20}$, then k only related with the polarization state, and the expression can be expressed as [10]

$$k = [1 - \sin^2 \theta \cdot \sin^2 (\Omega_{r-s}/2)]^{1/2} \quad (5)$$

Where θ is related to the polarization of incident light, Ω_{r-s} is decided by the birefringence of the fiber-optic interferometer's two arms.

From the formula (5), we know that the visibility changes from 0 to 1 when the birefringence of fiber-optic interferometer changes randomly. The change lead to the decline of the interference signal which is also known as the phenomenon of 'polarization-induced signal fading' caused by the instability of the polarization state of light in a single mode fiber [11]. The reasons for the instability of this polarization state are the internal factors of the fiber itself and some other external factors. The internal factor usually refers to the birefringence of the waveguide shape and the stress which induced by the distortion of fiber-optic cross-section geometry and the fiber itself, respectively. External factors will cause the fiber's anisotropy. They include some random excitations such as bending, twisting and vibration, or some environments of strong electric field, magnetic field and changing temperature.

In practice, the above situation is inevitable, so a new type of polarization-independent fiber-optic interferometer need to be designed [12]. The core part of the interferometer presented in this paper is the SFOP as shown in Fig. 1. It consists of a single-mode fiber, a ball convex lens and a fiber-optic self-focusing lens which is coated with a 'half transparent and half reflecting'

membrane (hereinafter referred to as membrane). The measured plane mirror is located at the focus of the ball convex lens. I_0 is the light intensity from the fiber end. It passes through the self-focusing lens and becomes parallel light when it is perpendicular to the end of the self-focusing lens, i.e. the membrane. I_0 is divided into two parts when gets to the membrane. One part is I_1 reflected from the membrane. The other arrives on the plane mirror through ball convex lens. Then it is reflected from the plane mirror and returns to the self-focusing lens through ball convex lens and the membrane in order. It is called I_2 here. So I_1 and I_2 meet completely the coherence and interfere perfectly with each other. At last the coherent light is transmitted through the same single-mode fiber and the polarization fading effect can be reasonably eliminated. This is called common-path transmission. Fig. 2 is the picture of the SFOP which is pasted on an iron piece. The fiber collimator's end and ball lens's diameter is only 1.8 mm.

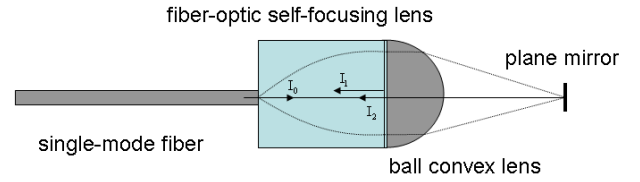


Fig. 1. Schematic diagram of the SFOP

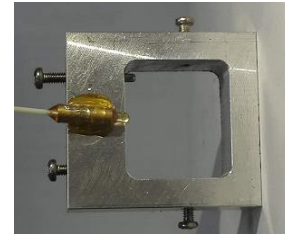


Fig. 2. Picture of the SFOP pasting on an iron piece

The structure of the SFOP has two advantages: On the one hand, a birefringent effect which produced by the influence of external environment is identical with the signal and reference light owing to the common-path transmission, so it eliminates effectively the polarization fading phenomena. On the other hand, the light will be collected and returned to the self-focusing lens which reflected by the plane mirror. So the second and more times' interference are suppressed perfectly, since the reflecting light will not be able to return to the fiber which comes from the surface of the ball convex lens.

It is supposed that the light field which passes from the fiber to the self-focusing lens and comes to the membrane is

$$\vec{E} = \vec{E}_0 e^{j(\omega t + \phi_0)} \quad (6)$$

Then the light field reflected from the membrane is

$$\vec{E}_1 = j\Gamma\vec{E}_0 e^{j(\omega t + \phi_0)} \quad (7)$$

The light field reflected back from the plane mirror is

$$\vec{E}_2 = j(1-\Gamma)\tau\vec{E}_0 e^{j(\omega t + \phi_0 + \phi_1 + \phi_s)} \quad (8)$$

\vec{E}_0 is the amplitude of the incident light, Γ is the reflection coefficient of the membrane, τ is the total loss coefficient for I_2 which produced during transmission, ϕ_0 is the initial phase of laser, ϕ_1 is the fixed phase difference generated by laser's transmission through the ball convex lens, $j = \exp(j\pi/2)$ indicates that the reflected light has a $\pi/2$ phase delay to the incident light. The propagation constant is $\beta = 2\pi/\lambda$ when the refractive index of air is 1. Ignoring of the fixed phase difference, the intensity of interference signal received from the detector is

$$I = |\vec{E}|^2 = I_1 + I_2 + 2\sqrt{I_1 I_2} \cos(\phi_s) \quad (9)$$

The phase ϕ_s is given by

$$\phi_s = \beta \cdot (2\Delta l) \quad (10)$$

Equation (9) shows that the interference signal received from detector is a function of the optical path difference for the two coherent beams. Equation (10) shows that the phase-shift ϕ_s is caused by the micro-displacement change Δl of the plane mirror along the direction of light propagation, so the micro-vibration measurement can be realized [13].

3. Experimental device

The PZT (piezoelectric ceramics) is used as the source of stable vibration signal to verify the fiber interferometer in the experiment. It will produce corresponding mechanical vibration when the two planes of polarization are put on alternating voltage. The micro-vibration will be elongated and shortened with the increasing and decreasing of the voltage. The measurement accuracy of micro-displacement can reach several nanometers. The schematic diagram for system is shown in Fig. 3. The picture of experimental system and devices is shown in Fig. 4. According to Fig. 3, its working principle is: the 1310 nm light beam emitted from laser injects into the optical fiber, passes through fiber circulator and then gets to the SFOP by leading fiber. Here the working principle of the SFOP is expounded in paragraph 2. The reflector mirror is fixed on the PZT and its displacement is controlled by PZT's

vibration [14]. The interference signal from the SFOP injects into leading fiber, passes through fiber circulator, and reaches the PIN photo detector. The voltage signal from PIN is transformed by analog-to-digital converter and processed by computer platform which made in National Instruments (NI) Corporation.

The interference fringe shows the cosine changes under the action of PZT. The phase of cosine function will produce 2π radian when the displacement of PZT elongated or shortened half wavelength, namely the fringe moved one. The phase-shift is the product of 2π and the voltage difference which corresponded to a complete sinusoidal wave. Accordingly the phase-shift coefficient $\Delta\phi/\Delta V$ of PZT can be easily obtained when the voltage ΔV of PZT and the changes of fringe are measured at the same time.

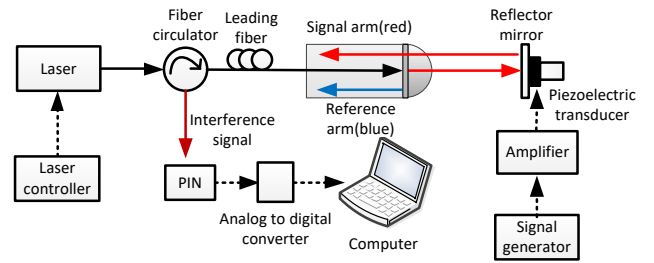


Fig. 3. Schematic diagram for experimental system

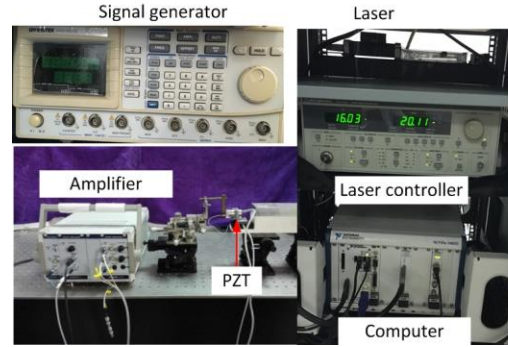


Fig. 4. Picture of experimental devices

4. Results and discussions

The measured interference signal is obtained as shown in Fig. 5: (a) as the interference signal in time domain; (b) as the corresponding spectral information. It can be seen from Fig. 5 that the SFOP can get good interference effect, and the interference fringes are very clear and stable. It is proved that the second and more times' interference are greatly suppressed for the introduction of the ball convex lens. We can clearly see the frequency-doubling signal generated by the periodic modulation from the corresponding frequency domain signal. The modulation frequency of the PZT is 3Hz.

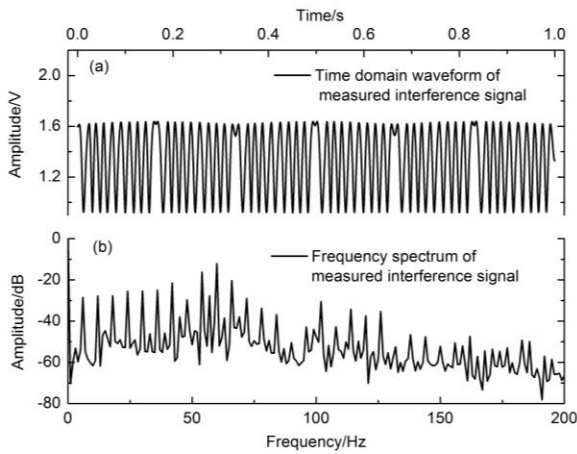


Fig. 5. Measured interference signal: (a) time domain signal, (b) frequency domain signal

The interference signals of the PZT with different amplitude of triangle wave driving voltage are collected. Fig. 6 is the measured triangle wave driving voltage signal and the corresponding interference signal. It can be clearly seen that the interference signal changed periodically with the triangle wave driving voltage changing periodically. The phase of sinusoidal wave is inverted at the turning point of voltage when it changes from increase to decrease or from decrease to increase.

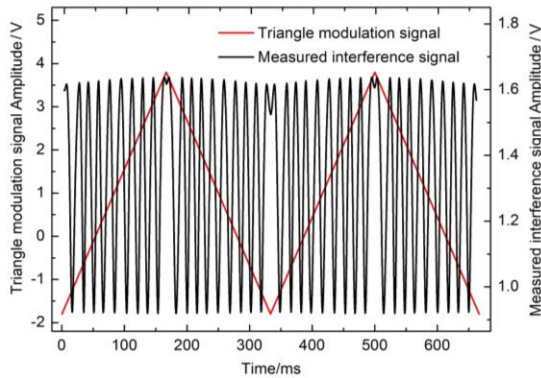


Fig. 6. Measured triangular wave driving voltage and corresponding interference signal

It is necessary to measure the phase shift coefficient which can reflect the stability of the working state of the interferometer [15]. The phase-shift coefficient should be fixed with the same PZT under different driving voltages about the stable interferometer. The smaller the fluctuation of phase-shift coefficient is, the more stable the working state of the interferometer is. PZT based on the inverse piezoelectric effect has high stability and repeatability which uses of closed-loop feedback control. In the experiment, the voltage signal of the triangular wave is gradually increased for the PZT, and the corresponding cosine curve of the interference fringe is

recorded. Then the phase-shift coefficient $\Delta\phi/\Delta V$ of the PZT is further obtained. Table 1 shows the phase-shift coefficient of the PZT under different amplitude of triangular wave voltage. The mean value and standard deviation of $\Delta\phi/\Delta V$ is 9.924 rad/V and 0.219 , respectively.

Table 1. Relationship between the driving voltage and the phase-shift coefficient of PZT

ΔV (V)	$\Delta\phi/\Delta V$ (rad/V)
3.0	9.9861
3.2	9.5677
3.4	9.6083
3.6	9.9355
3.8	9.8169
4.0	10.1407
4.2	10.2422
4.4	10.1078
4.6	9.9788
4.8	9.8587

Fig. 7 shows the phase-shift of PZT under different amplitude of triangle wave driving voltage. As a whole the voltage and phase-shift showed good linear relationship. The equality of $\Delta\phi = 10.286 \cdot \Delta V - 2.454$ is obtained by the least square method which is used for linear fitting. The correlation coefficient and standard deviation is 0.99834 and 0.29689 , respectively. The X axis represents the magnitude of the voltage applied to the PZT, and the Y axis represents the amount of phase changes. The slope of fitting line is the phase-shift coefficient 10.286 rad/V of PZT which is in good agreement with that obtained in Table 1. The results show that the polarization-independent fiber-optic interferometer designed has good stability. The error is mainly due to the hysteresis of PZT [16].

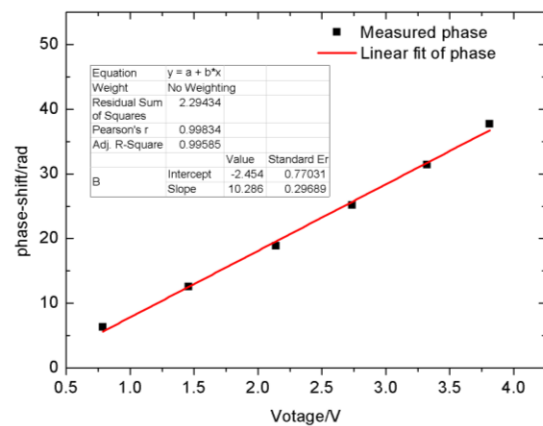


Fig. 7. Relation curve between driving voltage ΔV and phase-shift $\Delta\phi$

5. Conclusions

In this paper, we described a novel miniaturized polarization-independent fiber-optic interferometer based on common-path transmitting. It appropriately meets the demand of accurate measurement technology for miniaturization and integration. Especially we presented a SFOP through which the second and more times' interference are greatly suppressed. At the same time, the theoretical modeling of the interferometer is established. An experimental platform for micro-vibration measurement is built. The phase-shift coefficient of the PZT is measured accurately which is 10.286 rad/V and the standard deviation is 0.29689. The experimental results show that the interferometer can be used to measure the micro-vibration. It also can be significantly used on the study of the ultra-precise vibration measurement of the machine, micro-mechanics, precise sensors, and so on.

Acknowledgments

This work is supported by the Commonweal Project from Science Technology Department of Zhejiang Province (No.2017C33005).

References

- [1] S. Binu, V. P. M. Pillai, N. Chandrasekaran, *Opt. Laser Technol.* **39**, 1537 (2007).
- [2] X. B. Hong, J. Wu, C. Zuo, et al., *Appl. Optics* **50**(22), 4333 (2011).
- [3] C. Wang, L. L. Xu, J. Zhu, et al., *Opt. Laser. Eng.* **86**, 125(2016).
- [4] A. D. Kersey, M. J. Marrone, A. Dandridge, *Electron. Lett.* **27**(7), 562 (1991).
- [5] L. J. Li, Q. Ma, M. Y. Cao, et al., *Sensor. Actuat. B-Chem.* **234**, 674 (2016).
- [6] M. S. Yoon, C. J. Kang, Y. G. Han, *J. Lightwave Technol.* **33**(12), 2585 (2015).
- [7] F. Xie, X. F. Chen, L. Zhang, *Opt. Laser. Eng.* **47**(11), 1301 (2009).
- [8] G. Huang, Y. He, Z. Xu, *Optoelectron. Adv. Mat.* **10**(11-12), 844 (2016).
- [9] F. Xie, Z. M. Chen, J. Y. Ren, et al., *Opt. Eng.* **48**(4), 043608-1 (2009).
- [10] A. D. Kersey, M. J. Marrone, A. Dandridge, et al., *J. Lightwave Technol.* **6**(10), 1599 (1988).
- [11] A. A. Kersey, M. J. Marrone, *Am. J. Obstet. Gynecol.* **191**(4), 1311 (1989).
- [12] E. A. Kuzin, N. Korneev, J. W. Haus, et al., *Opt. Commun.* **183**, 389 (2000).
- [13] D. A. Jackson, A. Dandridge, S. K. Sheem, *Opt. Lett.* **5**(4), 139 (1980).
- [14] M. Yasin, Samian, F. N. Aini, *Optoelectron. Adv. Mat.* **10**(5-6), 347 (2016).
- [15] X. Chen, Y. Painchaud, K. Ogusu, H. Li, *J. Lightwave Technol.* **28**(14), 2017 (2010).
- [16] C. Ai, J. C. Wyant, *Appl. Optics* **26**(6), 1112 (1987).

*Corresponding author: hpmei@aiofm.ac.cn